Title
Redox Fluctuations Control the Coupled Cycling of Iron and Carbon in Tropical Forest Soils

Journal
Environmental Science and Technology, 52(24)

ISSN
0013-936X

Authors
Bhattacharyya, Amrita
Campbell, Ashley N
Tfaily, Malak M
et al.

Publication Date
2018-12-18

DOI
10.1021/acs.est.8b03408

Peer reviewed

Redox Fluctuations Control the Coupled Cycling of Iron and Carbon in Tropical Forest Soils

Amrita Bhattacharyya,[†,‡] Ashley N. Campbell,[‡] Malak M. Tfaily,[§] Yang Lin,[∥] Ravi K. Kukkadapu,[§] Whendee L. Silver,[∥] Peter S. Nico,[†] and Jennifer Pett-Ridge*[,‡]

† Earth and Environmental Sciences Area, Lawrence Berkeley National Laboratory, 1 Cyclotron Road, Berkeley, California 94720, United States

‡ Physical and Life Sciences Directorate, Lawrence Livermore National Laboratory, 7000 East Avenue, Livermore, California 94550, United States

§ Environmental Molecular Sciences Laboratory, Pacific Northwest National Laboratory, Richland, Washington 99354, United States

∥ Department of Environmental Science, Policy, and Management, University of California, Berkeley, Berkeley, California 94720, United States

*J. Pett-Ridge. E-mail: pettridge2@llnl.gov.

Abstract

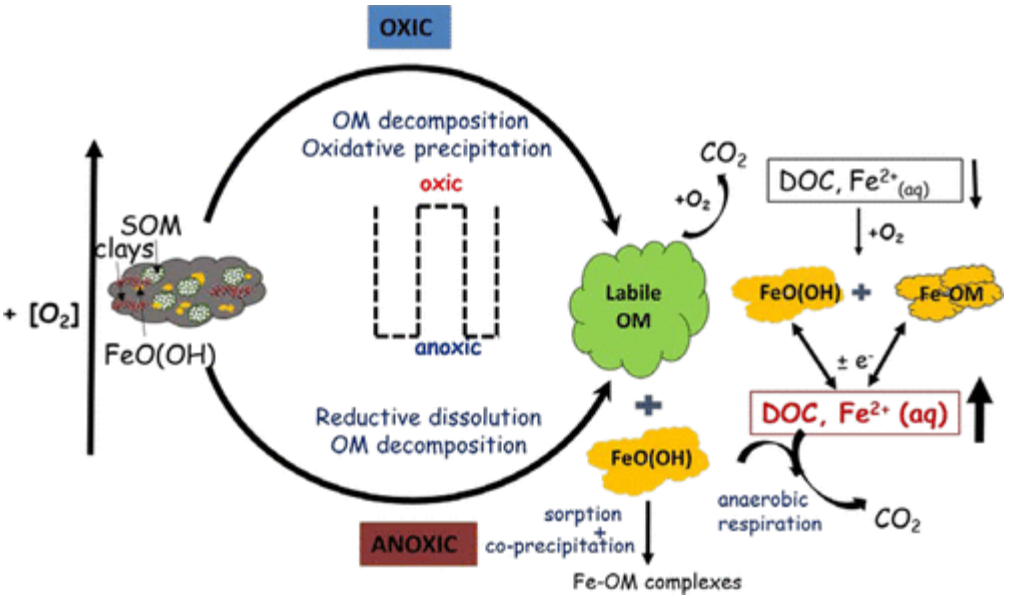

Oscillating redox conditions are a common feature of humid tropical forest soils, driven by an ample supply and dynamics of reductants, high moisture, microbial oxygen consumption, and finely textured clays that limit diffusion. However, the net result of variable soil redox regimes on iron (Fe) mineral dynamics and associated carbon (C) forms and fluxes is poorly understood in tropical soils. Using a 44-day redox incubation experiment with humid tropical forest soils from Puerto Rico, we examined patterns in Fe and C transformations under four redox regimes: static anoxic, “flux 4-day” (4d oxic, 4d anoxic), “flux 8-day” (8d oxic, 4d anoxic) and static oxic. Prolonged anoxia promoted reductive dissolution of Fe-oxides, and led to an increase in soluble Fe(II) and amorphous Fe oxide pools. Preferential dissolution of the less-crystalline Fe pool was evident immediately following a shift in bulk redox status (oxic to anoxic), and coincided with increased dissolved organic

C, presumably due to acidification or direct release of organic matter (OM) from dissolving Fe(III) mineral phases. The average nominal oxidation state of water-soluble C was lowest under persistent anoxic conditions, suggesting that more reduced organic compounds were metabolically unavailable for microbial consumption under reducing conditions. Anoxic soil compounds had high H/C values (and were similar to lignin-like compounds) whereas oxic soil compounds had higher O/C values, akin to tannin- and cellulose-like components. Cumulative respiration derived from native soil organic C was highest in static oxic soils. These results show how Fe minerals and Fe–OM interactions in tropical soils are highly sensitive to variable redox effects. Shifting soil oxygen availability rapidly impacted exchanges between mineral-sorbed and aqueous C pools, increased the dissolved organic C pool under anoxic conditions implying that the periodicity of low-redox events may control the fate of C in wet tropical soils.

Introduction

Humid tropical forest soils frequently alternate between fully oxygenated and anaerobic conditions, making them biogeochemical “hotspots” for redox reactions.(1−6) In the wet tropics, soils are often dominated by iron (Fe) and aluminum (Al)-rich oxide and hydr(oxide) clays that sorb organic carbon (OC), but are also susceptible to redox-induced mineral transformations.(6−10) The rapid Fe and C cycling typical of wet tropical ecosystems is fueled by a characteristically dynamic redox environment driven by high biological O_2 demand, high moisture (limiting O_2 diffusion), warm temperatures and abundant labile C. Unlike classically defined low-redox soils (e.g., wetlands)(11) where redox zonation can be relatively static in time and space, redox oscillations in upland tropical forest soils are spatially and temporally heterogeneous, likely occurring at the individual aggregate scale and responding rapidly (hourly to daily)(6,12,13) to variations in rainfall and dissolved organic carbon (DOC) inputs.

Iron minerals play a critical role in the C cycle of highly weathered tropical soils, particularly where frequent cycles of reduction and oxidation fuel a large portion of decomposition (~50% of C oxidation),(1−3,14−17)catalyzed by large Fe reducer populations (up to 10^9 per gram) that may be responsible for approximately 40% of soil CO_2 respiration.(7) Iron minerals also mediate belowground C retention(4,18−22) by binding organic matter (OM) in surface complexes and aggregates.(9,23−26) This is particularly true for high surface area, short range-ordered (SRO) Fe minerals (often a combination of ferrihydrite and nanoparticulate goethite), which are associated with some of the oldest C in terrestrial systems.(27,28) Much of the soil organic carbon (SOC) which is stabilized via Fe–OM associations is susceptible to redox effects because Fe can easily solubilize and reprecipitate/crystallize in response to local E_h conditions.(10,24) In an oscillating redox environment, when O_2 is periodically depleted, Fe minerals quickly become dominant terminal electron acceptors and are reduced. This primarily microbially mediated process can then liberate associated material

(nutrients or OM),(29,30) and we expect this liberated OM to rapidly appear in the dissolved OM pool. Previous work in Hawaiian tropical soils suggest Fe mineralogy evolves more quickly to a crystalline end point in sites where soil redox is variable, due to preferential dissolution of less crystalline materials during repeated reduction phases.(6,9,10) High surface area SRO Fe phases are likely produced by rapid mineral precipitation events and localized at redox interfaces in the soil profile. Yet, these same mineral phases are susceptible to rapid Fe reduction when O_2 becomes limiting, and this, in turn, may lead to C oxidation and increased C mobility (via colloid dispersion).(8,31)

In the coming 50 years, our study site, the US Forest Service Luquillo Experimental Forest (LEF) (within the El Yunque National Forest of northeastern Puerto Rico) is predicted to experience shifts in rainfall and temperature(32,33) that may significantly affect both soil moisture and the periodicity of soil redox oscillations. Multiple microbial/mineral driven processes could be affected, including OM degradation, methanogenesis, denitrification, and Fe reduction/oxidation,(34−43) because soil moisture regulates these key redox-sensitive aspects of the soil C cycle.(4) We expect that a shift to warmer, drier, more oxygenated soil conditions would strongly impact mineral-organic interactions (e.g., Fe–OM associations).(6,8−10,38,39,43) However, the degree to which Fe-oxides associate with SOM in tropical forest soils, particularly under oscillating redox conditions, is not well-understood and more information is needed on how adsorbed and coprecipitated SOM impacts biological Fe reduction and secondary Fe mineralization. In the LEF soils, the relationship between rainfall, soil moisture and soil redox is complex;(5,44) rainfall initially brings aeration, yet persistently high soil moisture causes diffusion limitations, and eventually anoxic conditions after soil microorganisms have scavenged available O_2. Indeed, in a study where experimental drought caused the soils to dry slightly (from 68% to 61% soil moisture) and become better aerated, the net effect caused lower soil CO_2 emissions.(35) Thus, to have a predictive understanding of wet tropical soil C and Fe cycling, what may be far more important than mean E_h (or mean soil [O_2]), is the pattern of redox oscillation, e.g., its periodicity (the recurrence rate of low-redox events) and duration (the persistence of low or high redox periods).

A better understanding of the influence of redox variability on Fe–OM relationships can help close mechanistic knowledge gaps in the tropical forest C cycle. Hence, in this study we sought to understand the impact of fluctuating redox conditions on Fe–OM interactions on humid tropical forest soils which were subjected to episodic oxidizing and reducing events. We used a replicated, high temporal resolution redox oscillation study, where soil moisture was held constant. We tested the hypothesis that the periodicity and duration of redox regimes would alter Fe speciation and the chemical composition of water extractable OM. Our results show how the nature of Fe–OM interactions changes in response to shifts in redox state,

which, in turn, impacts the coupled Fe–C biogeochemical cycle in humid tropical forest soils.

Materials and Methods

Study Site and Soil Sampling

Our study site in the LEF is part of the NSF sponsored Critical Zone Observatory and Long-Term Ecological Research programs (Lat. 18°18 N; Long. 65°50′ W) and characterized by steep topography, with naturally dynamic soil redox regimes.(4,5) The soils are highly weathered oxisols derived from volcaniclastic minerals (clay rich) that experience frequent soil O_2 depletion every 14–16 days (mean O_2 is 13 ± 0.21%, oscillating between 3 and 17%).(4,5) The mean water content is 35–65% and the pH is approximately 4.8.(45) Notably, LEF soils are enriched in SRO mineral phases that are highly susceptible to Fe reduction. Surface soils (0–10 cm) were collected from a slope location near the LEF El Verde field station in late January 2016 and shipped overnight to LLNL under ambient conditions. Once in the laboratory, soils were gently homogenized and visible plant debris, rocks, and soil macro-fauna were removed manually.

Redox Oscillation Experiment

Our experimental scheme for manipulating bulk soil redox followed previously established methods;(38) approximately 20 g (oven dry weight) of soil was weighed into a 500 mL glass microcosm; a total of 128 replicate microcosms were established. Microcosms were subjected to a 16-day pretreatment period to overcome disturbance effects associated with soil handling and homogenizing. Microcosms were capped with gastight lids fitted with a GeoMicrobial septa (Geo Microbial Technologies, Ochelata OK) with tygon tubing extending into the interior of the jar. To control the bulk soil redox conditions, either medical grade air (oxic) or nitrogen gas (anoxic) was delivered to the bottom of each jar at 3 mL min^{-1} and vented with a syringe needle in the septa. All microcosms were initially treated with 4 days of oxic conditions, followed by 4 days of anoxic (one complete redox cycle); this cycle was repeated once more during the pretreatment period. Microcosms were then divided into four redox regime treatments: (1) static anoxic, (2) static oxic, (3) 4 days oxic/4 days anoxic (flux 4-day), (4) 8 days oxic/4 days anoxic (flux 8-day), and incubated for 44 days, with 3 replicates per treatment and harvest point (and 5 replicates at the final harvest point). Microcosm headspace was manipulated in the same way as in the pretreatment. Flux 4-day and flux 8-day treatments started and ended with an oxic headspace.

Microcosm Harvests

During the experiment, replicate microcosms from all four redox treatments were destructively harvested on days 12, 20, 23, 36, and 44 (plus additional flux 4-day and flux 8-day microcosm harvests on days 16 and 33). For the two fluctuating redox treatments (flux 4-day and flux 8-day), microcosms

were harvested with an intensive time schedule, i.e., samples were collected immediately prior to the headspace gas switch (0 min), at 30 min postswitch, and then at 180 min in order to capture short-term geochemical responses that occurred as a function of the changing soil redox status. For these flux 4-day and flux 8-day treatments, data were grouped in two categories, oxic-to-anoxic switches (“reduction” events) and anoxic-to-oxic (“oxidation” events). In total, four reduction events and four oxidation events took place during the entire experiment. During harvest points, microcosm jars were opened, soils were lightly homogenized and then subsampled for microbial and chemical analyses. Sampling and extractions for anoxic headspace microcosms were performed within an anoxic chamber (5% H_2 and 95% N_2). All chemical reagents used within this chamber were prepared in advance with degassed water to preserve the Fe oxidation state, and for samples harvested at anoxic sampling points subsequent extractions were conducted under strict anoxic conditions.

pH, Moisture Content and Fe Chemical Forms

Soil pH was determined in a 100:1 slurry of Milli-Q water (18.2 Ω).(46) Moisture content and dry weight volume were determined from fresh and oven dry (105 °C) weights. Amorphous Fe (AO-Fe) was determined using acid ammonium oxalate extraction at pH ~ 3.(47) Soluble and weakly adsorbed Fe(II) was measured using 0.5 M HCl extraction followed by colorimetric estimation at 562 nm using the ferrozine method.(48) Additional extraction details are provided in the Supporting Information (SI).

Fe Speciation by X-ray Absorption Spectroscopy

Iron oxidation state and chemical coordination environment was determined using Fe K-edge extended X-ray absorption fine structure (EXAFS) (7112 eV) at beamline 4-3 at the Stanford Synchrotron Radiation LightSource at Menlo Park, CA, under ring operating conditions of 3 GeV with a current of 450 mA. EXAFS data were processed and analyzed using the Sixpack and Athena software packages.(49,50) Linear combination fitting (LCF) of spectra was performed in Athena in k^3-weighted k-space between $k = 2$ and 12, using the following end-members: siderite ($FeCO_3$), 2-and 6-line ferrihydrite [$Fe(OH)_3{\cdot}nH_2O$], goethite (α-FeOOH), lepidocrocite (γ-FeOOH), hematite (α-Fe_2O_3), pyrite (FeS_2), mackinawite (FeS), magnetite (Fe_3O_4), Illite, nontronite and ferrosmectite (Fe-containing clays). These references were chosen based on their likelihood to be present in our experimental samples. Compounds were only included in the fit if the fractional contribution was greater than 0.05. Additional details for the EXAFS analysis are presented in the SI.

Fe Speciation by Mössbauer Spectroscopy

To determine the changes in Fe speciation due to redox incubation, Mössbauer spectra were collected at multiple temperatures (298, 225, 140, 77, and 12 K) on pretreatment and static anoxic soils harvested at the end of

our incubation (44 days). Data was collected with a Web Research Company (St. Paul, MN) instrument at Pacific Northwest National Laboratory that included a closed-cycle cryostat (SHI-850, Janis Research Company, Inc., Wilmington, MA), a Sumitomo CKW-21 He compressor unit (Allentown, Pennsylvania), and a Ritverc (St. Petersburg, Russia) NaI detection system. A ^{57}Co/Rh source was used as the gamma energy source. Sample preparation was carried out in an anoxic chamber to prevent changes in Fe oxidation state. Data acquisition and data processing followed procedures reported in Peretyazhko et al., 2013.(51) Additional details on Mössbauer analysis are provided in the SI.

Estimation of Water-Extractable Dissolved Organic Carbon (DOC) Content

Water-extractable DOC was extracted by shaking 2.0 g of soil (dry weight equivalent) in 200 mL of Milli-Q water (18.2 Ω) for 1 h at 80 rpm. Suspensions were filtered through 0.45 μm nylon membrane filters using vacuum filtration. The filtrate was analyzed for dissolved organic carbon using a Shimadzu (Japan), Total Organic Carbon Analyzer (TOC-vcsh) at Lawrence Berkeley National Laboratory.

FT-ICR-MS Data Acquisition and Data Analysis

Samples were prepared for Fourier-transform ion-cyclotron-resonance mass spectrometry (FT-ICR-MS) according to Tfaily et al. 2017(52) (additional details are provided in the SI). Ultrahigh resolution characterization of water-extractable DOC was carried out using a 12T FT-ICR-MS at Pacific Northwest National Laboratory (Bruker SolariX, Billerica, MA). Water extracts were thawed overnight at 4 °C and diluted with methanol to improve electrospray ionization efficiency (no precipitation was observed). Suwannee River Fulvic Acid standard, obtained from the International Humic Substance Society, was used as a control and injected after every 20 samples, followed by a methanol blank to ensure instrument stability and verify no sample carryover. Samples were injected directly into the instrument using an automated custom-built system, and ion accumulation time was optimized for all samples, depending on the DOC concentration of the samples. Optimal parameters were established prior to the sample injection.(53−55) Additional FT-ICR-MS analytical information is presented in the SI.

The nominal oxidation state of carbon (NOSC) was calculated using the stoichiometry of each assigned formula for each organic compound identified in the water extracts.(56) The relevance of thermodynamic limitations under variable redox conditions can be evaluated by monitoring NOSC values as a function of the soil redox status. Partial least-squares discriminant analysis (PLS-DA) plots, generated by Metaboanalyst,(57) were used to illustrate the separation of specific metabolite classes based on the sample redox status. Details about this method are included in the SI. Organic compounds that were significantly different between treatments (i.e., organic compounds with a VIP (variable importance in projection) score >1 obtained from PLS-DA analysis were further examined in van-Krevelen diagrams and assigned to

major biochemical classes based on molar H:C (y-axis) and O:C (x-axis) ratios.(52) These compounds were clustered into three groups: (1) high O/C and H/C, in the carbohydrate region of a van-Krevelen diagram; (2) compounds with medium O/C and low H/C, in the aromatic region of a van-Krevelen diagram; and (3) compounds with medium O/C and H/C, in the lignin region of a van-Krevelen diagram.

CO_2 Flux Measurements

To measure microcosm carbon dioxide (CO_2) emission rate, headspace gas samples were collected immediately before microcosms were harvested for geochemical and microbial analyses. To make CO_2 flux measurement, microcosms were temporarily sealed for ~2 h, and 30 mL of headspace was collected both before and after the sealed period and stored in pre-evacuated 20 mL serum bottles. Gas samples were always collected from the subset of microcosms designated for the final harvest (on day 44, $n = 5$). For treatments with oscillating redox conditions, the CO_2 flux sealed period occurred prior to switching the microcosm headspace (redox state). CO_2 concentrations of gas samples were measured with a gas chromatograph (GC-14A, Shimadzu, Columbia, MD) equipped with a thermal conductivity detector. The average CO_2 flux during the sealed period was calculated using the increase in CO_2 concentration divided by the duration of the sealed period.

Statistical Analyses

Statistical analyses were performed with JMP software (SAS Institute Inc., Cary, North Carolina).(58) We tested our data sets (pH, water extractable DOC, AO-Fe and 0.5 M HCl extractable Fe(II)) for normality using the Shapiro-Wilk test. Response variables that did not meet assumptions of normality and homoscedasticity were log transformed. Analysis of variance and Tukey pairwise comparison tests were used to test for time and treatment effects on pH, DOC, AO-Fe and 0.5 N HCl extractable Fe(II) concentrations. We used a paired Wilcox test to indicate significant differences for each Fe species, pH, and DOC before and after switches in bulk redox conditions. Significance was determined at $p < 0.05$ unless otherwise noted.

Results and Discussion

pH and Moisture Content

Soil pH values did not change significantly as a function of redox treatment during the experiment (Figure S1a; Table S1) and averaged 5.63 ± 0.03. Moisture content also remained constant and was maintained at approximately 60% throughout the experiment.

Long-Term Effects of Redox Shifts on Fe and DOC Chemistry

Iron(II) concentrations extracted with 0.5 M HCl represent adsorbed and soluble phase Fe(II),(59) and in the LEF soil, initially averaged 0.005 ± 0.0003 g kg^{-1} soil (Figure 1a). Consistent anoxic conditions (static anoxic

treatment) led to a significant accumulation of Fe(II) relative to the other redox treatments (Figure 1a) that persistent throughout our study (even at day 20, where Fe(II) briefly dropped for unknown reasons). In contrast, Fe(II) was generally low in soils from the fluctuating treatments and mean concentrations were not statistically different from those in the static oxic soils ($p > 0.05$) (Table S1). However, the soil's current redox state when harvested (controlled via headspace gas composition) did have a significant impact on its 0.5 M HCl extractable Fe(II) concentration. This was particularly evident during the initial 23 days of the experiment; Fe(II) concentrations were significantly higher in soils sampled under an anoxic phase than under oxic conditions (e.g., days 16 and 23 for the flux 4-day, and days 12, 23 for flux 8-day) ($p = 0.04$ and $p < 0.0001$, respectively). When harvested during an oxic phase, Fe(II) concentrations in the fluctuating treatment soils were statistically similar to those of the static oxic soils. Overall, Fe(II) concentrations in the static oxic soils were consistently low and did not vary significantly, averaging 0.1 ± 0.01 g kg^{-1} soil.

Figure 1. Changes in (a) 0.5 M HCl-extractable Fe(II); (b) oxalateextractable Fe (AO-Fe); and (c) water-extractable dissolved organic carbon (WEDOC) concentrations (g kg−1 soil) in wet tropical soils (LEF, Puerto Rico) incubated with four redox treatments for 44 days. Concentrations for static anoxic, static oxic, flux 4-day, flux 8-day treatments are shown compared to the initial pretreatment concentration. Error bars indicate standard error for three replicate measurements (5 replicates at day 44). Anoxic sampling time points within the flux 4-day and flux 8-day treatments are indicated by filled symbols.

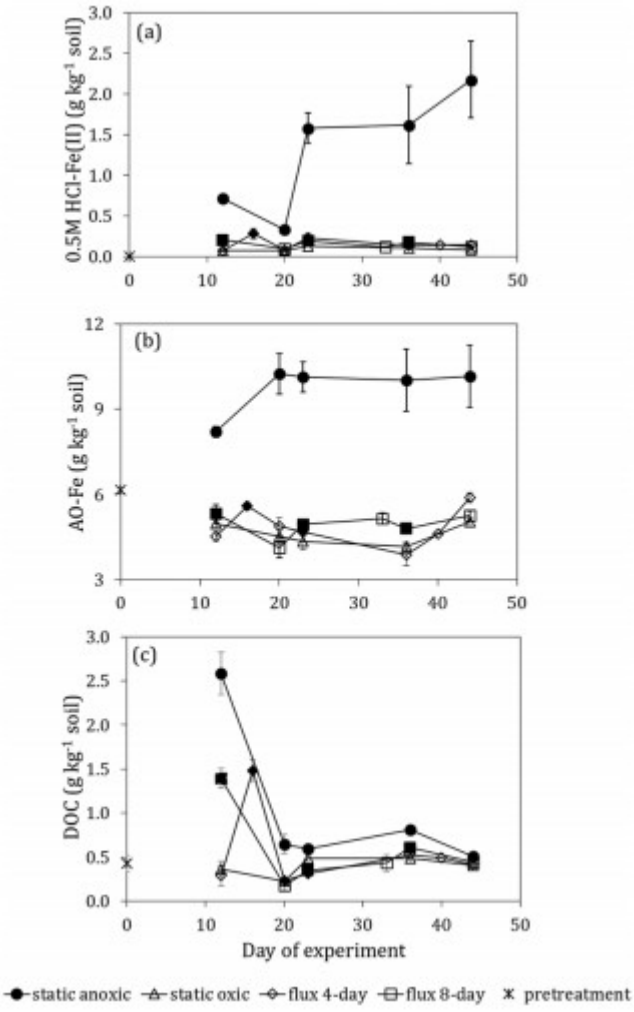

Ammonium oxalate-extractable Fe (AO-Fe, reflecting the amorphous or SRO Fe(oxy)hydroxide pool) was significantly higher in static anoxic soils relative to the other treatments ($p < 0.0001$, Figure 1b, Table S1), averaging 9.80 ± 0.40 g kg^{-1} soil. In the fluctuating redox soils, AO-Fe concentrations were low and relatively stable, although during the first half of our experiment, AO-Fe was significantly higher in the soils collected during an anoxic phase relative to soils collected during an oxic period ($p < 0.001$) of the flux 4-day treatment. Averaged across the entire incubation, AO-Fe concentrations from soils of fluctuating treatments were not statistically different from the low concentrations measured in the static oxic soils (Table S1).

As a complement to our solution chemistry measurements, bulk Fe K-edge EXAFS provides semiquantitative information regarding the different Fe forms present under the different redox conditions we investigated (Table1, Figure S2). For the fluctuating treatment soils, Fe-EXAFS analyses of bulk Fe mineralogy did not differ between the oxic and anoxic sampling time points, hence the Fe-EXAFS data presented here is from samples harvested at the end of the experiment, for each of our four redox treatments. Irrespective of redox regime, SRO ferrihydrite-like species were the dominant Fe mineral

present in these soils (Table1, Figure S2). Besides this SRO Fe-oxide pool, pretreatment and static anoxic soils had features akin to Fe(II)-bearing pyrite (FeS_2; 8–14%), while in the fluctuating and static oxic soils, goethite (a crystalline Fe-oxide [α-FeO(OH)]) was the major Fe mineral. We compared the radial structure functions (RSFs) of soils from our four redox treatments with pure Fe minerals to determine the local Fe coordination environment (Figure S2B). Structural features in the second Fe coordination shell (2.3–3.3 Å) indicate that the static anoxic soils were similar to ferrihydrite, whereas the fluctuating and static oxic soils had relatively higher crystallinity and paired more appropriately with goethite. These finding are similar to Thompson et al. (2006), who worked in wet tropical Hawaiian soils(6) and also found that Fe oxide crystallinity increased during soil redox fluctuations. Intriguingly, our EXAFS observations mirror our wet chemistry data, where Fe concentrations in fluctuating treatment soils most closely resembled those from the static oxic treatment. We expect that SRO ferrihydrite detected via bulk Fe-EXAFS should represent a similar pool to the oxalate-extractable Fe (AO-Fe). However, we note the AO-Fe fraction may also include other poorly crystalline minerals such as nanoparticulate goethite, as suggested by our Mossbauer data in the following section.

Table 1. Linear Combination Fit (LCF) Analysis Results for Fe K-Edge EXAFS Spectra of Wet Tropical Soils Incubated under Four Redox Treatments[a]

soil	ferrihydrite	goethite	pyrite	*R*-factor	reduced chi-square (χ^2)
	% contribution			(%)	
pretreatment	**74.4**[b]	17.6	8.0	0.10	0.02
static anoxic	**86.7**	0	13.3	0.31	0.01
flux 4-day	**74.2**	25.8	0	0.09	0.01
flux 8-day	**73.1**	26.9	0	0.15	0.01
static oxic	**58.5**	41.5	0	0.20	0.01

[a]Four treatments: static oxic, static anoxic, and two oscillation regimes. Data presented here are from soil samples collected at the end of a 44-day redox incubation study. The percentage of Fe species is based on linear combination fitting of Fe EXAFS spectra using the following phases: ferrihydrite, goethite, pyrite, magnetite, and siderite. [b]Values in bold are majority components, as identified by linear combination fits.

We used Mössbauer spectroscopy to provide greater details about the Fe-oxide pool. In general, Mössbauer spectral features of Fe-oxide are sensitive to Al-content, crystallinity/particle size, and magnitude of C and Si coatings, because these changes affect spectral features and can be difficult to identify by EXAFS. Spectra were obtained at various temperatures because at room temperature (298 K), clay Fe(III), Fe(II)-sulfides, and SRO Fe-oxides (e.g., ferrihydrite, nanoparticulate (np) goethite) containing different Al and organic coatings display a similar doublet feature. Mössbauer spectra at 225, 150, and 77 K, hence, was selected for data interpretation. At 225 K: (a) pure np-goethite displays a distinct sextet (Figure S3, right panel) and (b) pretreatment and day 44 anoxic samples exhibit different spectral features

(Figure S3) – at other temperatures there is little or no difference. Modeling of the 225 K spectra for pretreatment and anoxic samples indicated two distinct SRO sextets (labeled np-/Al-G1 and np-/Al-G2) of varying particle size, crystallinity and/or Al-content, and a doublet (Figure 2, Table S2). Comparison of 225 modeling to 150 and 77 K analysis (not shown) revealed the 225 K doublet to be a composite signal of np-Al/-G3, ferrihydrite-like, clay Fe(III), and Fe(II)-sulfides. Combined np-/Al-goethite (20.3%) and ferrihydrite-like mineral (8.7%) contents of the static anoxic sample were relatively higher than the pretreatment sample which had 11% and 8.4% np-/Al-goethite and ferrihydrite, respectively. The higher percentage of these minerals in the anoxic soil suggests sorbed C may have inhibited ferrihydrite reduction, making this Fe-pool less bioavailable.(60) This is in agreement with Chen et al.'s study in similar soils, which shows that Fe-oxidation and reduction rates affect Fe compositional phases using Mossbauer analysis.(61)

Figure 2. Modeled Mössbauer spectra (at 225 K) of soils from (a) pretreatment (oxic) and (b) static anoxic conditions for humid tropical soils from Puerto Rico. Mössbauer spectra shows the presence of multiple pools of Fe (shown by different line colors) and changes in spectral features (higher doublet content in the anoxic sample) with anoxic incubation. The line symbols used are as follows: blue = np-/Al-G1; red = np-/Al-G2; brown = adsorbed Fe(II); green = mixture of np-/Al-G3, ferrihydrite ("ferr"), iron sulfide (such as pyrite) and structural Fe(II). np-/Al-G1, np-/Al-G2 and np-/Al-G3 are nanoparticulate or Al-substituted goethite of varying crystallinities.

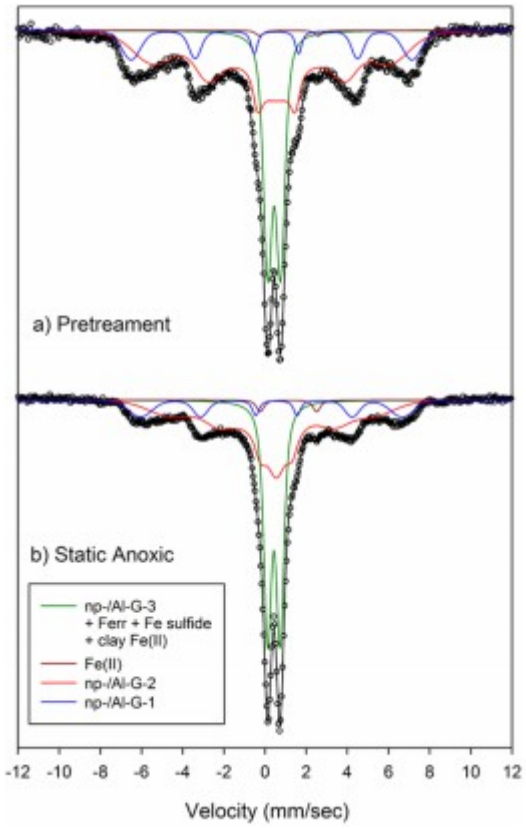

In a wet tropical soil, water-extractable DOC represents the organic C most available for microbial respiration and may include both dissolved and colloidal fractions.(62) In the LEF soil, DOC initially averaged 0.42 ± 0.09 g kg^{-1} (Figure 1c) and was significantly impacted by the redox treatments we imposed. Soils sampled during anoxic harvest points from the flux 4-day and flux 8-day treatments had significantly higher DOC concentrations (0.94 ± 0.05 g kg^{-1} soil) relative to those sampled under oxic conditions (0.36 ± 0.04 g kg^{-1} soil) ($p < 0.0001$). Overall, DOC concentrations for soils from the flux 4-day treatment were not significantly different from those from the static anoxic soils at $p = 0.05$ (Table S1), whereas soils from the flux 8-day treatment had generally lower DOC concentrations and were statistically similar to the mean value in the static oxic soils (Table S1). This suggests that the duration of exposure to oxic versus anoxic conditions can create significant differences in the DOC pool and highlights how the pattern of redox oscillation can affect bioavailable C in humid tropical forest soils. We note that near the end of our experiment, water extractable DOC concentrations for all four redox treatments converged around 0.44 ± 0.02 g kg^{-1} soil, implying an overall decline in labile C availability. This was likely caused by a lack of continued new C inputs, which in the natural system would continue to be provided (via ongoing decomposition and distribution following rainfall events).

Taken together, our results support the notion that alternating reductive Fe dissolution and precipitation events are a primary mechanism facilitating Fe–OM interactions under dynamic redox conditions in tropical soils.(6,10,63−65) While this process can be mediated by abiotic electron exchange pathways, it is also catalyzed by microbial metabolic activity.(66) In our LEF soils, we presume that abiotic reactions are steadily ongoing, such as preferential associations between SRO Fe-oxides and −O or −S containing organic ligands (e.g., oxalate or thiol) within the soils' polyfunctional organic matter.(18,64,67−70) Our EXAFS results suggest that prolonged anoxia in these tropical soils promotes the reductive dissolution of a portion of this SRO Fe-oxide pool, releasing soluble and weakly adsorbed Fe(II) which then can potentially bind to available organic molecules. This could explain the positive correlation we observe between reactive Fe-oxide phases and DOC under anoxic conditions ($r^2 = 0.4$), and indicates how Fe-oxides can regulate the availability of OC via coprecipitation or direct chelation.(71) It is also possible that decomposition of protected SOM occurred within microsites in the oxic soils, which when subjected to anoxic conditions, led to its solubilization and subsequent release as DOC.(72) However, this reaction can also be microbially driven, and interestingly, we observed a shift in bacterial community composition under prolonged anoxia that enriched for more taxa capable of iron-cycling (parallel study by A. N. Campbell, data not shown). The lower AO-Fe concentrations we observed in our fluctuating and static oxic treatments suggests a depletion of the kinetically labile Fe(III)-oxide pool when the soils are exposed to O_2. Finally, the presence of

crystalline long-range ordered goethite (α-FeOOH) in our fluctuating redox soils is congruent with the observation that alternate dissolution and precipitation accelerates transformation of metastable ferrihydrite to more thermodynamically stable phases.(64,68,73) These Fe dynamics parallel the increased Fe crystallinity Thompson et al. (2006) observed following redox oscillations in Fe(oxy)hydroxide-rich tropical soils of Hawaii(6,8) and show how Fe dynamics also regulate the availability of DOC.

Short-Term Redox Shifts: Effects on Fe and DOC Chemistry

In addition to examining longer-term trends in Fe(II), AO-Fe and DOC concentrations, we also assessed short-term effects, on the scale of minutes to hours, following redox changes within our soils (Figure 3). Soils from the flux 4-day and flux 8-day treatments exhibited surprisingly dramatic chemical changes soon after we changed bulk redox conditions. Since the trends for the flux 4-day and flux 8-day treatment soils were statistically indistinguishable, we present the average 0.5 N HCl extractable Fe(II), AO-Fe and water extractable DOC concentrations for these two treatments combined in Figure 3. For all three soil metrics, concentrations increased significantly within 30 min after a reduction event (switching from oxic to anoxic conditions) ($p < 0.001$). The opposite trend was observed during oxidation events, where 0.5 M HCl Fe(II) and water-extractable DOC dropped significantly ($p = 0.02$). AO-Fe concentrations also declined considerably during oxidation events, although were more variable and the change was not statistically significant at $p = 0.05$ (Figure 3, Table S3b).

Figure 3. Changes in 0.5 M HCl-extractable Fe(II) [top], oxalate-extractable Fe [middle] and water-extractable DOC [bottom] concentrations (in g kg^{-1} soil) immediately following soil reduction (oxic to anoxic) and oxidation (anoxic to oxic) events. Blue and red circles indicate oxic and anoxic time points, respectively. Error bars indicate standard error for three replicate measurements. Levels not connected by the same letter (A or B) are significantly different.

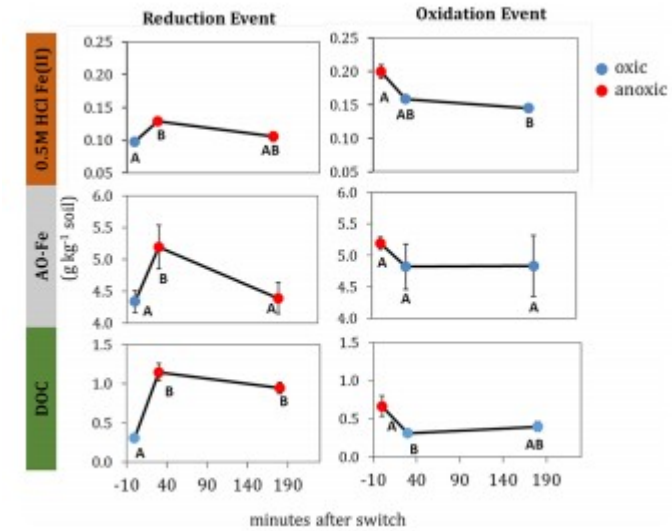

We hypothesized that the frequency of low-redox transition events controls exchanges of C between mineral-sorbed and aqueous pools in redox-dynamic tropical soils. This, in turn, likely affects whether labile C is lost as CO_2 or via leaching during redox transitions. The dramatic increase in water-extractable DOC content that we observed within 30 min of a reduction event implies that this DOC pool becomes available for respiration near-immediately after a change in redox state (and vice versa). As we have suggested above, the rapid increase in labile Fe and DOC pools at the onset of anoxic conditions is attributable to the reductive dissolution of crystalline Fe oxides and the accumulation of soluble Fe(II) and AO-Fe during the anoxic phase. DOC/Fe(II) and DOC/AO-Fe for the reduction and oxidation events, which give a quantitative comparison between rate of reduction of Fe and release of OC (Table S3), also point out how these two processes occur simultaneously during redox events. This is most likely due to direct OM release from dissolving Fe(III) mineral phases, though could also be related to acidification (we observed a pH decline of ~0.2 units during reduction events when DOC concentration increased almost 3-fold) (SI Figure S1b).(1,2,8) These striking short-term changes in soil chemistry suggest that repeated redox shifts may promote higher nutrient and elemental cycling than would be expected under more prolonged oxic (or anoxic) conditions. To our knowledge, these are some of the first results showing such rapid changes as fast as 30 min in solution chemistry due to short-term soil redox shifts in natural soil samples and hence comparison of our data set with previous studies was not feasible.

Effects of Redox Shifts on the Chemical Composition of Water-Extractable DOC

To assess the dominant classes of metabolites that developed during our four soil redox regimes, we investigated the chemical composition of the water-extractable DOC pool with FT-ICR-MS high resolution mass spectrometry.(74) Although our soils began the incubation with the same extractable metabolite composition (pretreatment), the fate of C (C speciation/composition) was highly dependent on soil redox regime. Calculations of the mean nominal oxidation state of carbon (NOSC) of soil metabolites extracted from each of our redox treatments help to identify differences in proportional abundance of major organic C classes, ranging from low NOSC (e.g., lipids) to high NOSC (e.g., sugars).(75) These NOSC values not only provide an indication of the biogeochemical availability of the DOC metabolite pool, but also the thermodynamic constraints placed on microbial decomposers who use these compounds as electron donors and a C source.(72) Soils from the anoxic treatment were dominated by compounds with more reduced C (more negative average NOSC) compared to those from both the fluctuating and static oxic treatments (Figure 4a–d). Soil NOSC status also changed with incubation time in each treatment; Figure 4a–d illustrates that in both the fluctuating treatments and the static oxic soils, NOSC values slowly increased with time, while soils from the static

anoxic treatment developed more and more reduced NOSC values. Comparison of the slopes from the flux 4-day, flux 8-day and static oxic treatments relative to the static anoxic showed differences at p = 0.09, 0.16 and 0.20, respectively. These results suggest that under anaerobic conditions, microbes leave behind low NOSC compounds which are thermodynamically less favored to sustain growth via anaerobic metabolism, particularly when coupled to Fe reduction.(72,76,77) For soils exposed to oxic conditions, whether consistently or only intermittently, microbial decomposers appear to have been less constrained by thermodynamic limitations, and favored decomposition of more reduced, high-energy yield compounds.

Figure 4. Average nominal oxidation state of carbon (NOSC) values based on Fourier-transform ion-cyclotron mass spectrometry (FT-ICR-MS) analysis of water extractable soil metabolites. Values were measured on a wet tropical forest soil incubated under four redox regimes over a 44-day redox incubation study. Plots a, b, c and d show NOSC values over the 44-day study for static oxic, flux 8-day, flux 4-day and static anoxic treatments, respectively. Plot e shows how the slope of NOSC trendlines (from plots a–d) varies as a function of soil redox treatment.

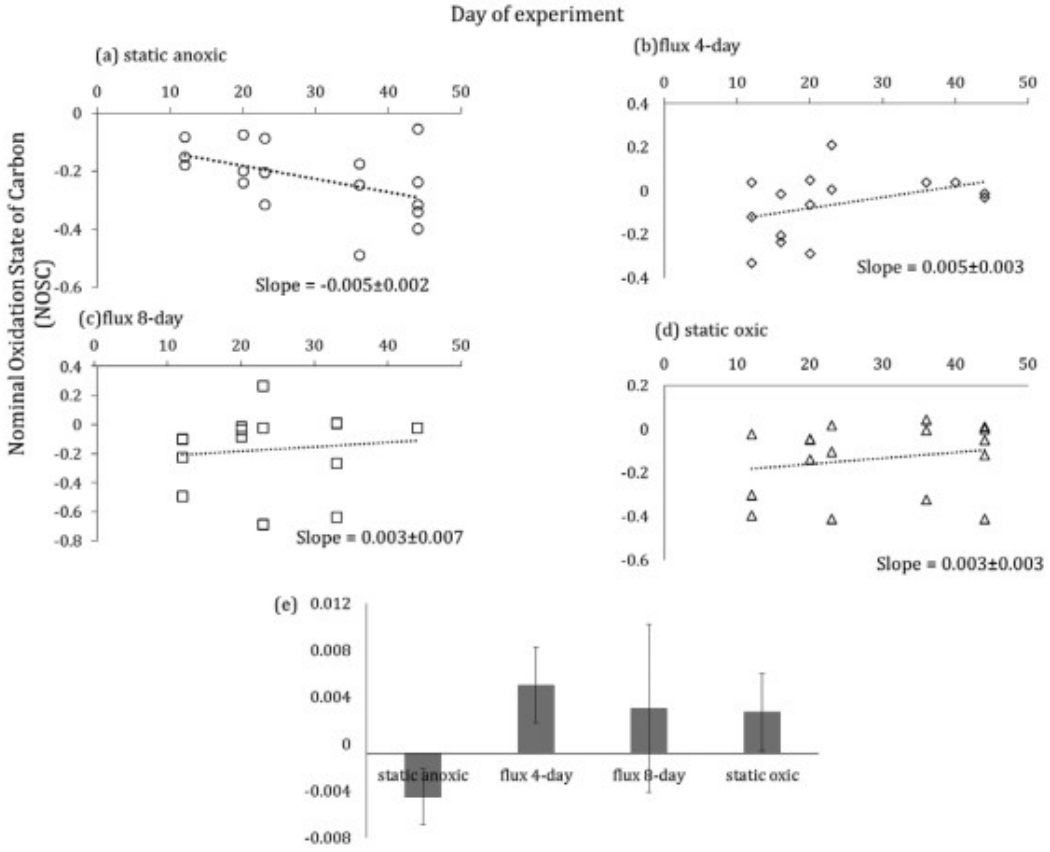

Analysis of FT-ICR-MS metabolite ordinations for the flux 4-day and flux 8-day treatments showed these treatments were not significantly different (Figure S4). As such, we combined them for further analysis and generated a principal components analysis plot (2D score plot) of the data as a function

of whether the sample was collected during an oxic vs anoxic time point (Figure 5a). The most significant differences between soil compounds harvested at an oxic vs anoxic time point were observed early in the experiment, suggesting that the most accessible compounds (both physically and chemically) were oxidized within 12 days of incubation; significant effects were not observed during the later harvest points. Van-Krevelen diagrams were created using the O/C and H/C ratios of the most significant organic compounds (Figure 5b) based on VIP-PLS-DA analysis (Figure S5). In general, unique water-extractable metabolites measured in the anoxic conditions had high H/C and low O/C values, and belong to the lignin-like class of compounds.(52) In contrast, unique metabolites detected under oxic conditions had high H/C and high O/C values, consistent with the carbohydrate-like region of the van-Krevelen diagram and low H/C and O/C consistent with aromatic-like region of the van-Krevelen diagram (Figure 5b). In addition to biotic limits on their degradation, we speculate that low O/C and moderate-to-low H/C metabolites may have been stabilized via association with Fe(oxy)hydroxide surfaces under anoxic conditions, further highlighting the important role of redox conditions on soil mineral-organic interactions. This is congruent with previous work which demonstrated that aromatic lignin molecules present under anoxic conditions are preferentially stabilized by amorphous Fe-oxide surfaces via sorption, forming lignin-ferrihydrite coprecipitates.(78−82) Under oxic conditions, lignin demethylation is thought to occur possibly via Fenton-like reactions where SOM oxidation is catalyzed by reactive oxygen species (ROS).(83,84) Overall, our FT-ICR-MS data suggest that water-extractable metabolite composition is highly dependent on the prevailing redox condition of these tropical soils.

Figure 5. (a) Principal components analysis (2D Score) plot of FT-ICR-MS data collected from samples harvested under anoxic (red circle) vs oxic (green circle) time points; and (b) van-Krevelen diagram (ratio of elemental H/C and O/C) of unique water extractable metabolites measured in soils harvested from oxic (green circle) and anoxic (red circle) conditions.

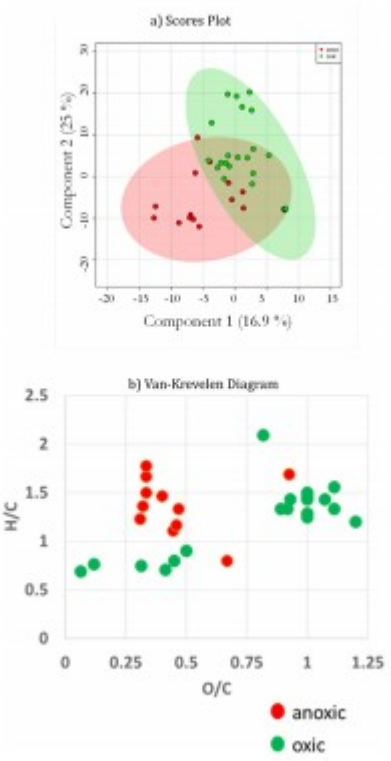

Soil CO_2 Emission under Variable Redox Conditions

We complemented our wet chemistry and molecular scale measurements of geochemical changes with macro-scale measurements of soil CO_2 fluxes (Figure S6). Soils from the static oxic treatment had significantly higher cumulative CO_2 fluxes than those from the flux 8-day treatment (Tukey's test: $p = 0.008$), but only marginally higher fluxes than the static anoxic ($p = 0.09$) and flux 4-day treatments ($p = 0.1$). Overall, redox regime effects on CO_2 flux were relatively small in amplitude, and we found little evidence that anoxia inhibited decomposition(85) in this system (as long as reductant remained available). This may be in part because these soils are known to contain an astonishing 10^9 Fe reducers in single gram (typical total bacterial cell concentrations are ~10^9).(86) It is estimated that this iron reducing bacterial community could alone support ~40% of total soil CO_2 respiration.(7) We speculate that availability of Fe(III) oxides as terminal electron acceptors,(87) or presence of aerobic microsites might also have influenced CO_2 production under anoxic conditions despite the protective effects of Fe–C interactions.(88) An interesting observation is that the sum of soluble Fe(II) and AO-Fe concentrations produced under static anoxic conditions do not quantitatively sum up to the amount of CO_2 which should be produced theoretically under anoxic conditions. This also points to the potential presence of alternate terminal electron acceptors such as manganese or nitrate, besides Fe in aerobic microsites under anoxic conditions. The increased CO_2 flux can also be attributed to the faster mineralization of certain C-containing functional groups which are in a positive oxidation state

(+3 for C in carboxylic group) as suggested by the NOSC data. A parallel spectromicroscopic investigation (data not shown) on the same soils showed that OM was preferentially sorbed to SRO Fe-oxides under anoxic conditions, this may have contributed to the slightly decreased CO_2 flux under anoxic conditions. Finally, reactive oxygen species (ROS) such as hydroxyl radicals have the potential to oxidize SOM, leading to CO_2 emissions and possibly low molecular weight, bioavailable products under fluctuating redox conditions.(1,44,63,89,90) While these latter processes serve as alternative mechanisms of CO_2 emission under variable redox conditions, from an ecosystem perspective, our results suggest that rapidly oscillating redox conditions may sustain soil respiration rates equivalent to those found under more aerated conditions.

Ecosystem Implications

The humid tropical forest soils of the Luquillo Experimental Forest in Puerto Rico frequently oscillate between oxic and anoxic periods.(5,33) Because predicted changes in global precipitation and temperature will likely shift the frequency, duration and degree of reduced conditions in tropical soils, we designed our study to evaluate whether these shifts might result in altered mineral-organic interactions and soil C cycling. Our results clearly illustrate that Fe–C coupling is a proximal controller of redox-driven biogeochemistry in these soils, includes electron transfer reactions (i.e., oxidation of C and reduction of Fe or other acceptors), and is sensitive to the frequency and duration of low redox intervals. We provide direct evidence that Fe–OM transformations in LEF soils are rapidly triggered by occasions where the bulk redox status of the soil is altered, events in the field that are known to occur on a daily to weekly basis(5) and are highly dependent on continued resupply of reduced organic matter. While our static treatments represent end members of bulk soil redox, and reflect uncommon redox regimes for the field, they are illustrative of the limitations imposed by nonoscillating conditions, for example what might be expected to occur following a prolonged drought (static oxic conditions).

Our results also indicate that C retention versus loss in redox-dynamic tropical soils is nonlinearly related to a soil’s average degree of oxygenation. Even brief reintroduction of oxygen can reset the balance of amorphous and more crystalline Fe phases, and facilitates microbial breakdown of reduced organic materials. Yet redox oscillations do not indefinitely promote rapid decomposition; without fresh inputs of organic matter or DOC, humid tropical soils may reach a tipping point and become far less responsive. Since the frequency of soil O_2 depletion also shapes microbial community structure and process rates,(37,39,43) we expect that in the field multiple C degradation pathways co-occur on relatively short timeframes (similar to the fast redox switches applied in our incubation), leading to a more rapid degradation of complex C substrates. Correspondingly, we expect that more frequent redox shifts might promote C loss from these soils via desorption and subsequent leaching of DOC.

To more accurately predict the ramifications of a warmer neotropical biome with more stochastic rainfall regimes, a mechanistic understanding of how different redox oscillation patterns affect biogeochemical mediation of C retention and loss pathways is critical.(91) Our findings suggest that soil redox cycling should be incorporated as a nonlinear predictive variable into models of wet tropical soil C cycling. The mechanistic understanding of Fe–OM interactions obtained from this study can be used to improve predictive mathematical models that forecast future tropical soil carbon balance and the design of future ecosystem scale studies.

Acknowledgments

We thank Daniel Nilson, Elizabeth Green, Jessica Wollard, Shalini Mabery, Rachel Neurath, Keith Morrison, Christopher Ward, Jeffery Kimbrel, Mona Hwang and Feliza Bourguet for assistance in the laboratory, and the Luquillo CZO and LTER for field infrastructure. This project was supported by a U.S. Department of Energy Early Career Award to J. Pett-Ridge (SCW1478) administered by the Office of Biological and Environmental Research (OBER), Genomic Sciences Program. Work at LLNL was performed under the auspices of the U.S. Department of Energy under Contract DE-AC52-07NA27344. CO_2 flux measurements contributed by W. Silver and Y. Lin were supported by NSF DEB-1457805, Luquillo CZO (EAR-1331841), LTER (DEB-0620910) and TES-DE-FOA-0000749. Synchrotron work was performed at beamlines 5.3.2.2 and 11.2.2 of the Advanced Light Source, which is a DOE Office of Science User Facility under contract no. DE-AC02-05CH11231. Use of the Stanford Synchrotron Radiation Lightsource, SLAC National Accelerator Laboratory, is supported by the U.S. Department of Energy, Office of Basic Energy Sciences under Contract No. DE-AC02-76SF00515. FT-ICR-MS and Mössbauer was performed using EMSL, a DOE Office of Science User Facility sponsored by OBER and located at Pacific Northwest National Laboratory (PNNL).

References

(1) Hall, S. J.; Silver, W. L. Iron oxidation stimulates organic matter decomposition in humid tropical forest soils. Global Change Biol. 2013, 19 (9), 2804−2813. (2) Hall, S. J.; Silver, W. L.; Timokhin, V. I.; Hammel, K. E. Lignin decomposition is sustained under fluctuating redox conditions in humid tropical forest soils. Global Change Biol. 2015, 21 (7), 2818− 2828. (3) Hall, S. J.; Silver, W. L.; Timokhin, V. I.; Hammel, K. E. Iron addition to soil specifically stabilized lignin. Soil Biol. Biochem. 2016, 98, 95−98. (4) Liptzin, D.; Silver, W.; Detto, M. Temporal Dynamics in Soil Oxygen and Greenhouse Gases in Two Humid Tropical Forests. Ecosystems 2011, 14 (2), 171−182. (5) Silver, W. L.; Lugo, A. E.; Keller, M. Soil oxygen availability and biogeochemistry along rainfall and topographic gradients in upland wet tropical forest soils. Biogeochemistry 1999, 44 (3), 301−328. (6) Thompson, A.; Chadwick, O. A.; Rancourt, D. G.; Chorover, J. Iron-oxide crystallinity increases during soil redox oscillations. Geochim. Cosmochim. Acta 2006, 70 (7), 1710−1727. (7) Dubinsky, E. A.; Silver, W. L.; Firestone, M. K. Tropical

forest soil microbial communities couple iron and carbon biogeochemistry. Ecology 2010, 91 (9), 2604−2612. (8) Thompson, A.; Chadwick, O. A.; Boman, S.; Chorover, J. Colloid mobilization during soil iron redox oscillations. Environ. Sci. Technol. 2006, 40 (18), 5743−5749. (9) Thompson, A.; Rancourt, D. G.; Chadwick, O. A.; Chorover, J. Iron solid-phase differentiation along a redox gradient in basaltic soils. Geochim. Cosmochim. Acta 2011, 75 (1), 119−133. (10) Tishchenko, V.; Meile, C.; Scherer, M. M.; Pasakarnis, T. S.; Thompson, A. Fe2+ catalyzed iron atom exchange and recrystallization in a tropical soil. Geochim. Cosmochim. Acta 2015, 148 (0), 191−202. (11) Ponnamperuma, F.; Tianco, E. M.; Loy, T. Redox equilibria in flooded soils: I. The iron hydroxide systems. Soil Sci. 1967, 103 (6), 374−382. (12) Pett-Ridge, J. Rapidly fluctuating redox regimes frame the ecology of microbial communities and their biogeochemical function in a humid tropical soil. Ph.D. Dissertation, University of California, Berkeley, Berkeley, 2005. (13) Reddy, K.; Patrick, W., Jr Effect of alternate aerobic and anaerobic conditions on redox potential, organic matter decomposition and nitrogen loss in a flooded soil. Soil Biol. Biochem. 1975, 7 (2), 87−94. (14) Barcellos, D.; Cyle, K. T.; Thompson, A. Faster redox fluctuations can lead to higher iron reduction rates in humid forest soils. Biogeochemistry 2018, 137 (3), 367−378. (15) Ginn, B. R.; Meile, C.; Wilmoth, J.; Tang, Y.; Thompson, A. Rapid iron reduction rates are stimulated by high-amplitude redox fluctuations in a tropical forest soil. Environ. Sci. Technol. 2017, 51 (6), 3250−3259. (16) Lalonde, K.; Mucci, A.; Ouellet, A.; Gelinas, Y. Preservation of organic matter in sediments promoted by iron. Nature 2012, 483 (7388), 198−200. (17) Parr, J.; Reuszer, H. Organic matter decomposition as influenced by oxygen level and method of application to soil. Soil Sci. Soc. Am. J. 1959, 23 (3), 214−216. (18) Kaiser, K.; Guggenberger, G. Sorptive stabilization of organic matter by microporous goethite: sorption into small pores vs. surface complexation. Eur. J. Soil Sci. 2007, 58 (1), 45−59. (19) Kaiser, K.; Mikutta, R.; Guggenberger, G. Increased Stability of Organic Matter Sorbed to Ferrihydrite and Goethite on Aging. Soil Sci. Soc. Am. J. 2007, 71 (3), 711−719. (20) Kögel-Knabner, I.; Guggenberger, G.; Kleber, M.; Kandeler, E.; Kalbitz, K.; Scheu, S.; Eusterhues, K.; Leinweber, P. Organo-mineral associations in temperate soils: Integrating biology, mineralogy, and organic matter chemistry. J. Plant Nutr. Soil Sci. 2008, 171 (1), 61−82. (21) Lutzow, M. v.; Kögel-Knabner, I.; Ekschmitt, K.; Matzner, E.; Guggenberger, G.; Marschner, B.; Flessa, H. Stabilization of organic matter in temperate soils: mechanisms and their relevance under different soil conditions - a review. Eur. J. Soil Sci. 2006, 57 (4), 426− 445. (22) Wagai, R.; Mayer, L. M. Sorptive stabilization of organic matter in soils by hydrous iron oxides. Geochim. Cosmochim. Acta 2007, 71 (1), 25−35. (23) Amstaetter, K.; Borch, T.; Kappler, A. Influence of humic acid imposed changes of ferrihydrite aggregation on microbial Fe(III) reduction. Geochim. Cosmochim. Acta 2012, 85 (0), 326−341. (24) Bhattacharyya, A.; Schmidt, M. P.; Stavitski, E.; Martínez, C. E. Iron speciation in peats: Chemical and spectroscopic evidence for the co-occurrence of ferric and ferrous iron in organic complexes and

mineral precipitates. Org. Geochem. 2018, 115, 124−137. (25) Cismasu, A. C.; Michel, F. M.; Tcaciuc, A. P.; Tyliszczak, T.; Brown, G. E., Jr. Composition and structural aspects of naturally occurring ferrihydrite. C. R. Geosci. 2011, 343 (2−3), 210−218. (26) Pedrot, M.; Le Boudec, A.; Davranche, M.; Dia, A.; Henin, O. How does organic matter constrain the nature, size and availability of Fe nanoparticles for biological reduction? J. Colloid Interface Sci. 2011, 359 (1), 75−85. (27) Mikutta, R.; Kleber, M.; Torn, M. S.; Jahn, R. Stabilization of soil organic matter: Association with minerals or chemical recalcitrance? Biogeochemistry 2006, 77 (1), 25−56. (28) Torn, M. S.; Trumbore, S. E.; Chadwick, O. A.; Vitousek, P. M.; Hendricks, D. M. Mineral control of soil organic carbon storage and turnover. Nature 1997, 389 (6647), 170−173. (29) Chacon, N.; Silver, W. L.; Dubinsky, E. A.; Cusack, D. F. Iron Reduction and Soil Phosphorus Solubilization in Humid Tropical Forests Soils: The Roles of Labile Carbon Pools and an Electron Shuttle Compound. Biogeochemistry 2006, 78 (1), 67−84. (30) Liptzin, D.; Silver, W. L. Effects of carbon additions on iron reduction and phosphorus availability in a humid tropical forest soil. Soil Biol. Biochem. 2009, 41 (8), 1696−1702. (31) Buettner, S. W.; Kramer, M. G.; Chadwick, O. A.; Thompson, A. Mobilization of colloidal carbon during iron reduction in basaltic soils. Geoderma 2014, 221, 139−145. (32) IPCC. The Fourth Assessment Report of the Intergovernmental Panel on Climate Change, Geneva, Switzerland, 2007. (33) O’Connell, C. S.; Ruan, L.; Silver, W. L. Drought drives rapid shifts in tropical rainforest soil biogeochemistry and greenhouse gas emissions. Nat. Commun. 2018, 9 (1), 1348. (34) Bouskill, N. J.; Lim, H. C.; Borglin, S.; Salve, R.; Wood, T. E.; Silver, W. L.; Brodie, E. L. Pre-exposure to drought increases the resistance of tropical forest soil bacterial communities to extended drought. ISME J. 2013, 7 (2), 384. (35) Bouskill, N. J.; Wood, T. E.; Baran, R.; Hao, Z.; Ye, Z.; Bowen, B. P.; Lim, H. C.; Nico, P. S.; Holman, H.-Y.; Gilbert, B.; et al. Belowground response to drought in a tropical forest soil. II. Change in microbial function impacts carbon composition. Front. Microbiol. 2016, 7, 323. (36) Bouskill, N. J.; Wood, T. E.; Baran, R.; Ye, Z.; Bowen, B. P.; Lim, H.; Zhou, J.; Nostrand, J. D. V.; Nico, P.; Northen, T. R.; et al. Belowground response to drought in a tropical forest soil. I. Changes in microbial functional potential and metabolism. Front. Microbiol. 2016, 7, 525. (37) DeAngelis, K. M.; Silver, W. L.; Thompson, A. W.; Firestone, M. K. Microbial communities acclimate to recurring changes in soil redox potential status. Environ. Microbiol. 2010, 12 (12), 3137−3149. (38) Pett-Ridge, J.; Firestone, M. K. Redox fluctuation structures microbial communities in a wet tropical soil. Appl. Environ. Microbiol. 2005, 71 (11), 6998−7007. (39) Pett-Ridge, J.; Petersen, D. G.; Nuccio, E.; Firestone, M. K. Influence of oxic/anoxic fluctuations on ammonia oxidizers and nitrification potential in a wet tropical soil. FEMS Microbiol. Ecol. 2013, 85 (1), 179−194. (40) Teh, Y. A.; Silver, W. L.; Conrad, M. E. Oxygen effects on methane production and oxidation in humid tropical forest soils. Global Change Biol. 2005, 11 (8), 1283−1297. (41) Templer, P. H.; Silver, W. L.; Pett-Ridge, J.; DeAngelis, K. M.; Firestone, M. K. Plant and microbial controls on nitrogen retention and loss in a humid tropical forest. Ecology 2008, 89 (11), 3030−

3040. (42) Wood, T. E.; Silver, W. L. Strong spatial variability in trace gasdynamics following experimental drought in a humid tropical forest. Global Biogeochem. Cycles 2012, 26, (3) DOI: 10.1029/ 2010GB004014. (43) Pett-Ridge, J.; Silver, W. L.; Firestone, M. K. Redox Fluctuations Frame Microbial Community Impacts on N-cycling Rates in a Humid Tropical Forest Soil. Biogeochemistry 2006, 81 (1), 95−110. (44) Hall, S. J.; McDowell, W. H.; Silver, W. L. When wet gets wetter: decoupling of moisture, redox biogeochemistry, and greenhouse gas fluxes in a humid tropical forest soil. Ecosystems 2013, 16 (4), 576−589. (45) White, A. F.; Blum, A. E.; Schulz, M. S.; Vivit, D. V.; Stonestrom, D. A.; Larsen, M.; Murphy, S. F.; Eberl, D. Chemical weathering in a tropical watershed, Luquillo Mountains, Puerto Rico: I. Long-term versus short-term weathering fluxes. Geochim. Cosmochim. Acta 1998, 62 (2), 209−226. (46) McLean, E. Soil pH and lime requirement. Methods of soil analysis. Part 2. Chemical and microbiological properties; American Society of Agronomy, Soil Science Society of America, 1982; pp 199− 224. (47) McKeague, J.; Day, J. Dithionite-and oxalate-extractable Fe and Al as aids in differentiating various classes of soils. Can. J. Soil Sci. 1966, 46 (1), 13−22. (48) Stookey, L. L. Ferrozine∂a new spectrophotometric reagent for iron. Anal. Chem. 1970, 42 (7), 779−781. (49) Ravel, B.; Newville, M. ATHENA, ARTEMIS, HEPHAESTUS: data analysis for X-ray absorption spectroscopy using IFEFFIT. J. Synchrotron Radiat. 2005, 12 (4), 537−541. (50) Webb, S. SIXpack: a graphical user interface for XAS analysis using IFEFFIT. Phys. Scr. 2005, 2005 (T115), 1011. (51) Peretyazhko, T.; Zachara, J. M.; Kukkadapu, R. K.; Heald, S. M.; Kutnyakov, I. V.; Resch, C. T.; Arey, B. W.; Wang, C. M.; Kovarik, L.; Phillips, J. L.; et al. Pertechnetate (TcO_4^-) reduction by reactive ferrous iron forms in naturally anoxic, redox transition zone sediments from the Hanford Site, USA. Geochim. Cosmochim. Acta 2012, 92, 48−66. (52) Tfaily, M. M.; Chu, R. K.; Toyoda, J.; Tolic, N.; Robinson, E.´ W.; Pasa-Tolicˇ , L.; Hess, N. J. Sequential extraction protocol for ´ organic matter from soils and sediments using high resolution mass spectrometry. Anal. Chim. Acta 2017, 972, 54−61. (53) Tfaily, M. M.; Hamdan, R.; Corbett, J. E.; Chanton, J. P.; Glaser, P. H.; Cooper, W. T. Investigating dissolved organic matter decomposition in northern peatlands using complimentary analytical techniques. Geochim. Cosmochim. Acta 2013, 112 (0), 116−129. (54) Tfaily, M. M.; Hodgkins, S.; Podgorski, D. C.; Chanton, J. P.; Cooper, W. T. Comparison of dialysis and solid-phase extraction for isolation and concentration of dissolved organic matter prior to Fourier transform ion cyclotron resonance mass spectrometry. Anal. Bioanal. Chem. 2012, 404 (2), 447−457. (55) Tfaily, M. M.; Podgorski, D. C.; Corbett, J. E.; Chanton, J. P.; Cooper, W. T. Influence of acidification on the optical properties and molecular composition of dissolved organic matter. Anal. Chim. Acta 2011, 706 (2), 261−267. (56) LaRowe, D. E.; Van Cappellen, P. Degradation of natural organic matter: a thermodynamic analysis. Geochim. Cosmochim. Acta 2011, 75 (8), 2030−2042. (57) Xia, J.; Sinelnikov, I. V.; Han, B.; Wishart, D. S. MetaboAnalyst 3.0∂making metabolomics more meaningful. Nucleic Acids Res. 2015, 43 (W1), W251−W257. (58) Sall, J.; Lehman, A.;

Stephens, M. L.; Creighton, L. JMP start statistics: a guide to statistics and data analysis using JMP. Sas Institute, 2012. (59) Fredrickson, J. K.; Zachara, J. M.; Kennedy, D. W.; Dong, H.; Onstott, T. C.; Hinman, N. W.; Li, S.-m. Biogenic iron mineralization accompanying the dissimilatory reduction of hydrous ferric oxide by a groundwater bacterium. Geochim. Cosmochim. Acta 1998, 62 (19), 3239−3257. (60) Chen, C.; Kukkadapu, R.; Sparks, D. L. Influence of coprecipitated organic matter on Fe2+ (aq)-catalyzed transformation of ferrihydrite: implications for carbon dynamics. Environ. Sci. Technol. 2015, 49 (18), 10927−10936. (61) Chen, C.; Meile, C.; Wilmoth, J. L.; Barcellos, D.; Thompson, A. Influence of pO2 on Iron Redox Cycling and Anaerobic Organic Carbon Mineralization in a Humid Tropical Forest Soil. Environ. Sci. Technol. 2018, 52 (14), 7709−7719. (62) Zsolnay, A. Dissolved organic matter: artefacts, definitions, and functions. Geoderma 2003, 113 (3−4), 187−209. (63) Hall, S. J.; Silver, W. L. Reducing conditions, reactive metals, and their interactions can explain spatial patterns of surface soil carbon in a humid tropical forest. Biogeochemistry 2015, 125 (2), 149−165. (64) Hansel, C. M.; Benner, S. G.; Neiss, J.; Dohnalkova, A.; Kukkadapu, R. K.; Fendorf, S. Secondary mineralization pathways induced by dissimilatory iron reduction of ferrihydrite under advective flow. Geochim. Cosmochim. Acta 2003, 67 (16), 2977−2992. (65) Hall, S. J.; Berhe, A. A.; Thompson, A. Order from disorder: do soil organic matter composition and turnover co-vary with iron phase crystallinity? Biogeochemistry 2018, 140 (1), 93−110. (66) Piepenbrock, A.; Schröder, C.; Kappler, A. Electron transfer from humic substances to biogenic and abiogenic Fe (III) oxyhydroxide minerals. Environ. Sci. Technol. 2014, 48 (3), 1656− 1664. (67) Bhattacharyya, A.; Stavitski, E.; Dvorak, J.; Martínez, C. E. Redox interactions between Fe and cysteine: Spectroscopic studies and multiplet calculations. Geochim. Cosmochim. Acta 2013, 122, 89− 100. (68) Deelman, J. Breaking Ostwald’s rule. Chem. Erde 2001, 61 (3), 224−235. (69) Kostka, J. E.; Luther, G. W. Partitioning and speciation of solid phase iron in saltmarsh sediments. Geochim. Cosmochim. Acta 1994, 58 (7), 1701−1710. (70) Sulzberger, B.; Suter, D.; Siffert, C.; Banwart, S.; Stumm, W. Dissolution of Fe (III)(hydr) oxides in natural waters; laboratory assessment on the kinetics controlled by surface coordination. Mar. Chem. 1989, 28 (1−3), 127−144. (71) Henneberry, Y. K.; Kraus, T. E.; Nico, P. S.; Horwath, W. R. Structural stability of coprecipitated natural organic matter and ferric iron under reducing conditions. Org. Geochem. 2012, 48, 81−89. (72) Keiluweit, M.; Wanzek, T.; Kleber, M.; Nico, P.; Fendorf, S. Anaerobic microsites have an unaccounted role in soil carbon stabilization. Nat. Commun. 2017, 8 (1), 1771. (73) Williams, A. G.; Scherer, M. M. Spectroscopic evidence for Fe (II)− Fe (III) electron transfer at the iron oxide− water interface. Environ. Sci. Technol. 2004, 38 (18), 4782−4790. (74) Tfaily, M. M.; Chu, R. K.; Tolic, N.; Roscioli, K. M.; Anderton,́ C. R.; Pasa-Tolicˇ , L.; Robinson, E. W.; Hess, N. J. Advanced solvent́ based methods for molecular characterization of soil organic matter by high-resolution mass spectrometry. Anal. Chem. 2015, 87 (10), 5206−5215. (75) Kim, S.; Kramer, R. W.; Hatcher, P. G. Graphical method for analysis of ultrahigh-resolution

broadband mass spectra of natural organic matter, the van Krevelen diagram. Anal. Chem. 2003, 75 (20), 5336−5344. (76) Boye, K.; Herrmann, A. M.; Schaefer, M. V.; Tfaily, M. M.; Fendorf, S. Discerning microbially mediated processes during redox transitions in flooded soils using carbon and energy balances. Front. Environ. Sci. 2018, 6, 15. (77) Boye, K.; Noel, V.; Tfaily, M. M.; Bone, S. E.; Williams, K. H.;¨ Bargar, J. R.; Fendorf, S. Thermodynamically controlled preservation of organic carbon in floodplains. Nat. Geosci. 2017, 10 (6), 415. (78) Chorover, J.; Amistadi, M. K. Reaction of forest floor organic matter at goethite, birnessite and smectite surfaces. Geochim. Cosmochim. Acta 2001, 65 (1), 95−109. (79) Kleber, M.; Sollins, P.; Sutton, R. A conceptual model of organo-mineral interactions in soils: self-assembly of organic molecular fragments into zonal structures on mineral surfaces. Biogeochemistry 2007, 85 (1), 9−24. (80) Rillig, M. C.; Caldwell, B. A.; Wösten, H. A.; Sollins, P. Role of proteins in soil carbon and nitrogen storage: controls on persistence. Biogeochemistry 2007, 85 (1), 25−44. (81) Eusterhues, K.; Neidhardt, J.; Hadrich, A.; Ku¨sel, K.; Totsche, K. U. Biodegradation of ferrihydrite-associated organic matter. Biogeochemistry 2014, 119 (1−3), 45−50. (82) Eusterhues, K.; Rennert, T.; Knicker, H.; Kögel-Knabner, I.; Totsche, K. U.; Schwertmann, U. Fractionation of Organic Matter Due to Reaction with Ferrihydrite: Coprecipitation versus Adsorption. Environ. Sci. Technol. 2011, 45 (2), 527−533. (83) DeAngelis, K. M.; Allgaier, M.; Chavarria, Y.; Fortney, J. L.; Hugenholtz, P.; Simmons, B.; Sublette, K.; Silver, W. L.; Hazen, T. C. Characterization of Trapped Lignin-Degrading Microbes in Tropical Forest Soil. PLoS One 2011, 6 (4), No. e19306. (84) Filley, T.; Cody, G.; Goodell, B.; Jellison, J.; Noser, C.; Ostrofsky, A. Lignin demethylation and polysaccharide decomposition in spruce sapwood degraded by brown rot fungi. Org. Geochem. 2002, 33 (2), 111−124. (85) Keiluweit, M.; Nico, P. S.; Kleber, M.; Fendorf, S. Are oxygen limitations under recognized regulators of organic carbon turnover in upland soils? Biogeochemistry 2016, 127 (2−3), 157−171. (86) Whitman, W. B.; Coleman, D. C.; Wiebe, W. J. Prokaryotes: The unseen majority. Proc. Natl. Acad. Sci. U. S. A. 1998, 95 (12), 6578−6583. (87) Sutton-Grier, A. E.; Keller, J. K.; Koch, R.; Gilmour, C.; Megonigal, J. P. Electron donors and acceptors influence anaerobic soil organic matter mineralization in tidal marshes. Soil Biol. Biochem. 2011, 43 (7), 1576−1583. (88) Keiluweit, M.; Bougoure, J. J.; Nico, P. S.; Pett-Ridge, J.; Weber, P. K.; Kleber, M. Mineral protection of soil carbon counteracted by root exudates. Nat. Clim. Change 2015, 5 (6), 588−595. (89) Yuan, X.; Davis, J. A.; Nico, P. S. Iron-mediated oxidation of methoxyhydroquinone under dark conditions: kinetic and mechanistic insights. Environ. Sci. Technol. 2016, 50 (4), 1731−1740. (90) Yuan, X.; Nico, P. S.; Huang, X.; Liu, T.; Ulrich, C.; Williams, K. H.; Davis, J. A. Production of hydrogen peroxide in groundwater at Rifle, Colorado. Environ. Sci. Technol. 2017, 51 (14), 7881−7891. (91) Treseder, K. K.; Balser, T. C.; Bradford, M. A.; Brodie, E. L.; Dubinsky, E. A.; Eviner, V. T.; Hofmockel, K. S.; Lennon, J. T.; Levine, U. Y.; MacGregor, B. J.; et al. Integrating microbial ecology into

ecosystem models: challenges and priorities. Biogeochemistry 2012, 109 (1−3), 7−18.